BESSE, J.-P., BOLTE, M., BAUD, G. & CHEVALIER, R. (1976). *Acta Cryst.* B**32**, 3045–3048.

COTTON, F. A. (1965). *Inorg. Chem.* **3**, 334–336.

COTTON, F. A. (1966). *Q. Rev. Chem. Soc.* **20**, 389–401.

COTTON, F. A. & HARRIS, C. B. (1965). *Inorg. Chem.* **3**, 330–333.

International Tables for X-ray Crystallography (1959). Vol. II. Birmingham: Kynoch Press.

International Tables for X-ray Crystallography (1974). Vol. IV. Birmingham: Kynoch Press.

LONGO, J. M. & SLEIGHT, A. W. (1968). *Inorg. Chem.* **7**, 108–111.

MORROW, N. L. & KATZ, L. (1968). *Acta Cryst.* B**24**, 1466–1471.

WALTERSSON, K. (1976). *Acta Cryst.* B**32**, 1485–1489.

WILHELMI, K. A., LAGERVALL, E. & MULLER, O. (1970). *Acta Chem. Scand.* **24**, 3406–3408.

Acta Cryst. (1978). B**34**, 3535–3542

Electron-Density Distribution in Crystals of $K_2Na[Co(NO_2)_6]$

BY S. OHBA, K. TORIUMI,* S. SATO AND Y. SAITO

The Institute for Solid State Physics, The University of Tokyo, Roppongi-7, Minato-ku, Tokyo 106, *Japan*

(*Received* 14 *April* 1978; *accepted* 4 *July* 1978)

The electron-density distribution in crystals of $K_2Na[Co(NO_2)_6]$ has been determined by the single-crystal X-ray diffraction method. The residual electron density around the Co atom in the octahedral complex ion, $[Co(NO_2)_6]^{3-}$, comprises the eight positive peaks arranged at the corners of a cube [1·69 (14) e Å^{-3} at 0·43 Å from Co] and the six negative peaks on the Co—N bond [−0·79 (13) e Å^{-3} at 0·62 Å from Co]. The central Co atom is largely neutralized, the number of electrons within a sphere of radius 1·22 Å (octahedral covalent radius of Co) being 26·3 (1). The valence-electron populations of the atoms were refined and the net charges of Co, N and O atoms were estimated to be +0·06 (6), −0·07 and −0·22 (2) e, respectively. A bonding peak with height 0·32 (10) e Å^{-3} is observed between the N and O atoms. The bonding electron in the N—O bond is largely extended perpendicularly to the plane of the nitro group, showing some π-bond character.

Introduction

The asphericity of non-bonding 3*d* electrons around the octahedrally coordinated transition-metal atoms has been observed for a number of compounds. All their coordination geometries are, however, more or less deformed from a regular octahedron, as shown in Table 1. Crystals of $K_2Na[Co(NO_2)_6]$ are cubic and the Co atoms lie on sites of T_h symmetry. Thus it may be possible to observe the asphericity of non-bonding *d* electrons in an exact cubic field. Another interest lies in the electron-density distribution in a nitro group. An attempt has been made to analyse the bond nature of the coordinated NO_2^- group in this compound.

* Present address: The Institute for Molecular Science, Myodaiji, Okazaki 444, Japan.

Experimental

Single crystals of $K_2Na[Co(NO_2)_6]$ were grown by the diffusion method at 5 °C. Two small beakers, one containing 0·7 g of $Na_3[Co(NO_2)_6]$ and the other 3·0 g of KCl crystals, were placed side by side in a 50 ml beaker and distilled water was poured very carefully down the walls of the beakers until the level was about 3 cm above the tops of the two small beakers. To prevent the evaporation of water, the large beaker was covered with a piece of paper, and kept in a

Table 1. *Symmetries of the complex ions and their first neighbours*

Complex ion	$[Co(NH_3)_6][Co(CN)_6]$(1)		$M^{II}_2SiO_2$(2)	TiO_2(3)	$K_2Na[Co(NO_2)_6]$(4)
	C_{3i}	C_{3i}	C_{3v}	D_{2h}	T_h
First neighbours	CoN_6	CoC_6	$M^{II}O_6$	TiO_6	CoN_6
	D_{3d}	D_{3d}	D_{3d}	D_{2h}	O_h

(1) Iwata & Saito (1973); for other references see Iwata (1977). (2) M^{II} = Ni, Fe and Co. (3) $Ti^{4+}(d^0)$. (4) Present study.

refrigerator. The crystals in the small beakers dissolved gradually in water and the solutes diffused in solution; after two weeks orange-red prismatic crystals were formed on the wall of the beaker containing the $Na_3[Co(NO_2)_6]$ solution. Some of the KCl crystals remained undissolved in the other small beaker. As is known, the composition of the precipitates obtained from a mixture of K^+ with $Na_3[Co(NO_2)_6]$ depends upon the Na^+/K^+ ratio; *i.e.*, the higher the Na^+/K^+ ratio in solution is, the higher is the ratio in the precipitates. In fact, a hexanitrocobaltate(III) salt with higher Na content than the stoichiometric formula, $K_2Na[Co(NO_2)_6]$, can be prepared (Ferrari, Cavalca & Coghi, 1955). The crystal data are listed in Table 2.

The crystal was ground into a sphere of about 0·2 mm in diameter. Intensity data were collected on a Rigaku automated four-circle diffractometer at 24 °C with Mo $K\alpha$ radiation monochromated by a graphite plate. A θ–2θ continuous scan technique was employed. Some other experimental conditions are summarized in Table 3. As the diffracted intensities decreased in the region of high 2θ values, the scan speed was slowed down stepwise according to the 2θ values. 20 weak reflexions in the low-angle region ($2\theta \leq 60°$) were remeasured at a lower scan speed (0·5° min^{-1}). In order to reduce the systematic errors, four symmetry-related reflexions were measured in the $2\theta \leq 90°$ range ($\sum ||F| - \langle |F| \rangle| / \sum |F| = 1{\cdot}6\%$). For 31 reflexions with $2\theta \leq 60°$ that showed poor agreement among symmetry-related members, some other symmetry-related reflexions were measured. A check of multiple reflexion was also carried out for questionable reflexions ($2\theta \leq 90°$) by rotating the net plane around the scattering vector at the reflecting position. The intensities of the five standard reflexions were measured every 50 to 20 measurements. During the period of data collection (23 days), the intensities of the standard reflexions decreased by 3·6%. Scaling of the observed structure amplitudes was made by reference to a series of intensities of the standard reflexions. The intensity measurement was performed up to 150° in 2θ, and 992 independent non-zero F values were obtained. The standard deviation of each reflexion was estimated from the equation: $[\sigma(|F|)]^2 = [\sigma(\text{count})]^2 + (k|F_o|)^2$. The proportionality factor k was given the value 0·013, which was obtained as follows: the intensity fluctuation of the incident beam was estimated to be 2·5 (1)% and this will cause an error of $0{\cdot}012|F_o|$ in $|F_o|$, and an error of $0{\cdot}0033|F_o|$ may be expected from the absorption correction (Toriumi, Ozima, Akaogi & Saito, 1978). The lattice constant was determined from 18 2θ values in the range $60 \leq 2\theta \leq 67°$.

Table 2. *Crystal data*

$K_{2(1-\alpha)}Na_{1+2\alpha}[Co(NO_2)_6]$, $\alpha = 0{\cdot}18$ (1)
Cubic, $a = 10{\cdot}245$ (1) Å, $U = 1075{\cdot}3$ (1) Å^3
Space group $Fm3$, $Z = 4$
μ(Mo $K\alpha$) = 24·4 cm^{-1}, $D_x = 2{\cdot}66$ g cm^{-3}

Table 3. *Experimental conditions*

Radius of crystal specimen	0·093 mm
Radiation	Mo $K\alpha$
Take-off angle	5°
Monochromator	Graphite plate
Scan mode	θ–2θ
Scan rate (θ)	2° min^{-1} ($2\theta \leq 60°$)
	1° min^{-1} ($60 < 2\theta \leq 90°$)
	0·5° min^{-1} ($90 < 2\theta \leq 150°$)
Maximum number of repetitions	2 ($2\theta \leq 60°$)
	3 ($2\theta > 60°$)
Criterion to terminate repetition	$\sigma(\|F\|)/\|F\| \leq 0{\cdot}003$
$2\theta_{max}$	150°
Number of measured symmetry-related members	4 ($2\theta \leq 90°$)
	1 ($2\theta > 90°$)
Number of observed independent reflexions	992

Refinement

The function minimized was $R_w(F) = [\sum w(|F_o| - |F_c|)^2 / \sum w|F_o|^2]^{1/2}$, where the weight w was defined by $w = 1/[\sigma(|F_o|)]^2$. The positional and thermal parameters were refined by the full-matrix least-squares program *RADIEL* (Yang, Becker & Coppens, to be published), as well as the valence-electron populations and valence-form factors (Iwata, 1977). The atomic form-factor table given by Fukamachi (1971) was used. An isotropic extinction correction was made and the smallest extinction factor was 0·94 for 400. The valence electrons were taken as indicated in Table 4. The net charge in the crystal was constrained to be zero.

In the ideal crystals of $K_2Na[Co(NO_2)_6]$, K^+ and Na^+ occupy the position 8(*c*) ($\frac{1}{4},\frac{1}{4},\frac{1}{4}$) and 4(*b*) ($0,\frac{1}{2},0$), respectively. The positional disorder between K^+ and Na^+ was taken into consideration, where the temperature factors were assumed to be equal for the different ions on the same sites. The population parameters and valence-electron populations were difficult to determine uniquely so that K and Na were fixed as ions of single positive charge. The refinement of site

Table 4. *Refinement of valence-electron populations*

	Core	Valence	Charge	κ
Co	Ar	$(4s)^2(3d)^7$	+0·06 (6)	1·02 (1)
N	He	$(2s)^2(2p)^3$	−0·07	1·02 (1)
O	He	$(2s)^2(2p)^4$	−0·22 (2)	0·99 (1)
K^+	Ar		+1	
Na^+	Ne		+1	

occupancy parameters indicated that the disorder occurs only in the position 8(*c*), and 4(*b*) is exclusively occupied by Na^+. A population parameter α, defined as $K_{2(1-\alpha)}Na_{(1+2\alpha)}[Co(NO_2)_6]$, was estimated to be 0·18 (1).

The parameters converged to their self-consistent values after the repetition of the following three steps. Firstly the positional parameters were determined from the high-order reflexions ($\sin\theta/\lambda \geq 0{\cdot}7$ Å^{-1}). In the second step, the thermal parameters, a scale factor and the population parameter α were refined simultaneously excluding 16 low-angle reflexions ($\sin\theta/\lambda \leq 0{\cdot}3$ Å^{-1}) affected considerably by the extinction effect. Normally the temperature factors as well as a scale factor should be determined with high-order reflexions, since they are expected to show less bias from valence-density distributions (Stevens & Coppens, 1975). But it was not appropriate in this case. For the reflexions ($\sin\theta/\lambda \geq 0{\cdot}7$ Å^{-1}) the scale factor was given the value 1·75. If the parameters were refined with the fixed scale factor of 1·75, an unreasonable result was obtained: the extinction parameter became negative. The reason for this failure may be partly due to inappropriate selection of high-order reflexions; however, it has not been fully understood. In the third step, the valence-electron populations, valence-form factors κ and the extinction parameter were refined on the basis of all the reflexions. The final $R_w(F)$ is 0·038, and some other refinement information is listed in Table 5.* The final parameters are given in Table 6. The interatomic distances and bond angles are listed in Table 7.

* A list of observed and calculated structure amplitudes has been deposited with the British Library Lending Division as Supplementary Publication No. SUP 33811 (10 pp.). Copies may be obtained through The Executive Secretary, International Union of Crystallography, 5 Abbey Square, Chester CH1 2HU, England.

Table 5. *Refinement information*

N_o (number of reflexions)	992
N_v (number of variables)	21
$S = [\sum w(\lvert F_o\rvert - \lvert F_c\rvert)^2/(N_o - N_v)]^{1/2}$	1·16
$R_w = [\sum w(\lvert F_o\rvert - \lvert F_c\rvert)^2/\sum w\lvert F_o\rvert^2]^{1/2}$	0·038
$R = \sum\lvert\lvert F_o\rvert - \lvert F_c\rvert\rvert/\sum\lvert F_o\rvert$	0·036

Results and discussion

Thermal motion

As seen from Table 6, the N atom oscillates nearly isotropically, whereas the O atoms exhibit considerably anisotropic thermal motion with the largest amplitude perpendicular to the NO_2 plane.

The thermal motion of the $[Co(NO_2)_6]^{3-}$ ion was analysed in terms of the isotropic rigid-body modes of translation (**T**) and libration ($\boldsymbol{\omega}$): the function minimized was $R_w = [\sum w(U_{obs} - U_{calc})^2/\sum wU_{obs}^2]^{1/2}$, where w stands for the atomic weight. The rigid-body motion of $Co(NO_2)_6$ is given by: $\mathbf{T} = 0{\cdot}010$ (4) Å^2, $\boldsymbol{\omega} = 7{\cdot}3$ (28) deg^2 and $R_w = 24{\cdot}6\%$. When the O atoms were excluded from the rigid-body analysis the rigidity considerably increased: $\mathbf{T} = 0{\cdot}0097$ (10) Å^2, $\boldsymbol{\omega} = 3{\cdot}9$ (14) deg^2 and $R_w = 6{\cdot}2\%$. This fact suggests librational motion of nitro groups around the Co—N bond. Accordingly an attempt was made to estimate the librational motion of the NO_2 group in the following way: if the components for the isotropic rigid-body motion of $Co(NO_2)_6$ are subtracted from the observed U_{ij} for the O atoms, those for the librational motion of NO_2, $(\omega_{11},\omega_{22},\omega_{33})$, will be obtained, where the centre of the vibration is fixed at the N atom $(0,y_N,0)$. Then we have four equations as follows (Cruickshank, 1956):

$$U_{11} - (\mathbf{T} + y^2\,\boldsymbol{\omega}) = \Delta U_{11} = y^2\,\omega_{33} \quad (1)$$

$$U_{22} - (\mathbf{T} + x^2\,\boldsymbol{\omega}) = \Delta U_{22} = x^2\,\omega_{33} \quad (2)$$

$$U_{33} - [\mathbf{T} + (x^2 + y^2)\,\boldsymbol{\omega}] = \Delta U_{33} = y^2\,\omega_{11} + x^2\,\omega_{22} \quad (3)$$

$$U_{12} - (-xy\boldsymbol{\omega}) = \Delta U_{12} = -xy\omega_{33} \quad (4)$$

where x, y and 0 give the atomic position of the O atom with respect to the N atom. The best fit value of ω_{33} for

Table 7. *Interatomic distances and bond angles with their estimated standard deviations in parentheses*

Co—N	1·9516 (7) Å	O···Na(1)	2·7619 (7) Å
N—O	1·2316 (9)	O···K(2)	2·9673 (4)
O—N—O	119·34 (7)°	N—O···Na(1)	97·69 (4)°

Table 6. *The final parameters*

The values of the positional and thermal parameters are multiplied by 10^5 and those of the populations by 10^3. The temperature factors (Å^2) are as follows: $\exp[-2\pi^2a^{*2}(h^2U_{11} + k^2U_{22} + l^2U_{33} + 2hkU_{12})]$.

	Population	x	y	z	U or U_{11}	U_{22}	U_{33}	U_{12}
Co		0	0	0	905 (4)			
N		0	19049 (7)	0	1460 (20)	1096 (17)	1391 (19)	0
O		10376 (8)	25119 (7)	0	1900 (20)	1620 (17)	3360 (31)	−570 (15)
Na(1)		0	50000	0	2345 (23)			
K(2)	822 (10)	25000	25000	25000	2232 (16)			
Na(2)	178							

Scale factor 1·817 (4).
Isotropic extinction parameter $g = 0{\cdot}27$ (17) $\times 10^3$.

(1), (2) and (4) is found to be 14·1 deg². ω_{11} and ω_{22}, however, cannot be determined uniquely and only one relation is given by (3), $\omega_{22} = -0{\cdot}34\omega_{11} + 42{\cdot}4$ (deg²). The value of ω_{11} may, however, be estimated to be in the range $0 \sim 6^2$ deg² judging from the value of ω_{33}, so that ω_{22} is *ca* 6^2 deg², indicating that the r.m.s. amplitude of rotation around the Co–N bond is about 6°. The results are given in Table 8. Such knowledge of the anisotropic thermal motion of each atom is of crucial importance in the discussion of the features of the final difference synthesis in a later section.

As described above the CoN_6 can be regarded as a rigid body; thus the N atom exhibits less thermal motion along the Co–N bond. On the other hand, Cullen & Lingafelter (1971) and Joesten, Takagi & Lenhert (1977) observed greater thermal motion of the N atoms along the Cu–N bond than at right angles to it in the cubic crystals of $K_2Pb[Cu(NO_2)_6]$ and these authors interpreted this unusual observation in terms of a dynamic Jahn–Teller effect. Our present result indeed supports their conclusion.

Electron population

The charge-refinement result listed in Table 4 indicates that the negative charge on $[Co(NO_2)_6]^{3-}$ is distributed on the 12 O atoms, and the Co atom is largely neutralized. From the direct integration of electron density, the number of electrons around the Co atom in a sphere of radius 1·22 Å (covalent radius of Co) is 26·3 (1), in accordance with Pauling's electroneutrality rule (Pauling, 1960). The standard deviations assigned to the number of electrons and to the deformation density were derived from the errors in the observed structure factors and an error in the scale factor of 0·2% (Toriumi & Saito, 1978).

Residual electron density

A three-dimensional difference synthesis was calculated using all the reflexion data with $\sin\theta/\lambda \leq 1{\cdot}36$ Å^{-1}, where the subtracted densities were calculated on the basis of spherical atoms with effective charges listed in Table 4. Fig. 1 shows a section of the final difference Fourier synthesis containing two threefold axes and a Co–N bond. A remarkable feature is the distribution of residual electron density around the Co nucleus. A sharp positive peak of 1·69 (14) e Å^{-3} is observed on the threefold axis at 0·43 Å from the Co atom. In all, eight equivalent peaks are arranged at the apices of a cube around the Co atom. A section containing a face of the cube is shown in Fig. 2. All the peaks are fused together with positive region along the cube edges (see Fig. 2.7 of Weiss, 1966). On the other hand, a negative peak of −0·79 (13) e Å^{-3} appears on the Co–N bond axis at 0·62 Å from the Co nucleus. These features around the Co atom are essentially the same as those observed for $[Co(NH_3)_6][Co(CN)_6]$ (Iwata & Saito, 1973), which indicates an excess electron density in the t_{2g} orbitals and a deficiency in the e_g orbitals. In Fig. 1, a maximum of 0·46 (15) e Å^{-3} is observed between the Co and N atoms at 1·43 Å from Co. The zero contour, chain-dotted in Fig. 1, encircles the Co nucleus, the radius of its cirumscribed circle being equal to the octahedral radius of Co. The bonding peak lies outside this region, in contrast to the case of $[Co(NH_3)_6]^{3+}$ where it lies at 1·21 Å from Co.

Fig. 3(*a*) shows a section of the difference synthesis through the plane of NO_2. A positive peak of 0·32 (10) e Å^{-3} appears on the N–O bond axis at 0·50 Å from the N atom. It may be an N–O σ-bonding peak. This peak lies within a sphere with the covalent radius of N (0·7 Å). The centre of the peak does not lie on the N–O bond axis. This peak position is seriously affected by the series termination as shown in Table 9, so that the deviation from the N–O bond axis may not be significant. On the extension of the N–O bond a positive peak appears and in the direction nearly perpendicular to the N–O bond two positive peaks are also observed.

Table 8. *Observed and calculated tensor elements of thermal vibration, U_{ij} (Å$^2 \times 10^4$)*

	Co	N			O			
	U	U_{11}	U_{22}	U_{33}	U_{11}	U_{22}	U_{33}	U_{12}
Observed	91	146	110	139	190	162	336	−57
Calculated*	97	143	97	143	176	110	190	−33
ΔU_{ij}					14	52	146	−24
Calculated†					17	49		−28

* Isotropic rigid-body thermal motion around the Co atom. R.m.s. amplitudes of translational and librational motions are 0·10 (3) Å and 2·0 (12)°, respectively.

† Librational motion of NO_2 group in its plane with the N atom fixed. R.m.s. amplitude is 3·8°.

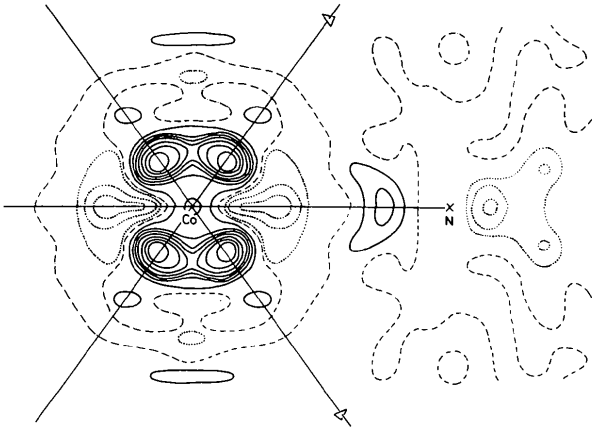

Fig. 1. Section of the final difference synthesis through a Co–N bond and two threefold axes. Contours are at intervals of 0·2 e Å^{-3}. Negative contours are dotted, zero being chain-dotted.

These deformation densities around the O atom may be explained by a simple molecular orbital model for NO_2^- as follows (see Fig. 4): the valence state of N may be described in terms of three similar hybrid orbitals, which can be formed by mixing the $2s$ orbital and the two $2p$ atomic orbitals, say $2p_y$ and $2p_z$. If these hybrids are denoted by h_1, h_2 and h_3, the appropriate N valence state must be $N(1s^2,h_1^2,h_2^1,h_3^1,2p_x^1)$. The relevant orbital on the O atom is the digonal hybrid formed by $2s$ and $2p_z$ (z referring to the N–O axis), and the valence state is $O(1s^2,h_1^1,h_2^2,2p_x^1,2p_y^2)$, where h_1 and h_2 denote the two lobes of the digonal hybrids. $O(h_2^2)$ forms a lone pair located at the rear of the O atom with respect to N. $O(2p_y^2)$ is also a lone pair and the lobes are perpendicular to the N–O axis and in the plane of the nitro group. The $N(h_2^1)$ orbital overlaps with $O(h_1^1)$ to form a σ bond and $N(2p_x^1)$ and $O(2p_x^1)$ overlap to form a π bond. An excess electron is in the other $O(2p_x)$ orbital as in the resonance formula drawn in Fig. 4. A peak with height 0·36 (11) e Å^{-3} on the extension of the N–O bond at 0·18 Å from O is spurious (see Fig. 8). Two peaks corresponding to $O(p_y^2)$ both lie at 0·53 Å from the O atom, but they have unequal peak heights, one being 0·17 (10) and the other 0·37 (10) e Å^{-3}. This unsymmetrical charge density may be accounted for by the electrostatic interaction with Na^+ that lies on a line bisecting the ONO angle and at 3·171 (1) Å from the N atom (see Fig. 7). One of the two lobes lying in the ONO angle is closer to Na^+ than the other, and is more stabilized, giving rise to the accumulation of more charge density. Fig. 5 shows a section of these two peaks through the O atom and

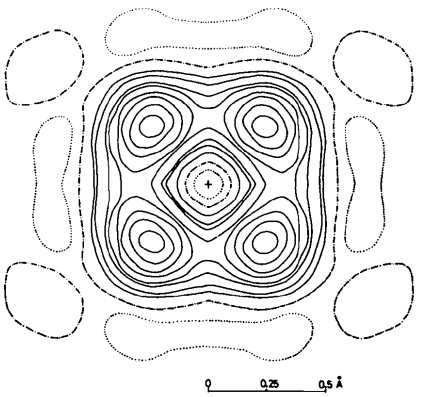

Fig. 2. Section of the difference synthesis through the plane perpendicular to the Co–N bond and at 0·246 Å from the Co. Contours are at intervals of 0·2 e Å^{-3}. The cross indicates the section of the Co–N bond.

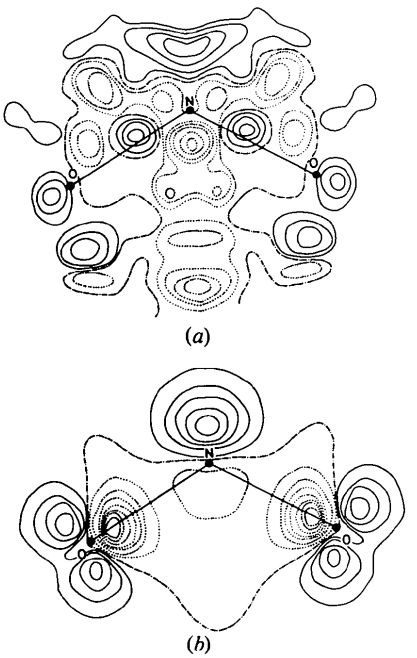

Fig. 3. Deformation density in the NO_2 plane. (*a*) X-ray difference Fourier map. (*b*) Theoretical map calculated by the CNDO/2 method. Contours are at intervals of (*a*) 0·1 and (*b*) 0·5 e Å^{-3}.

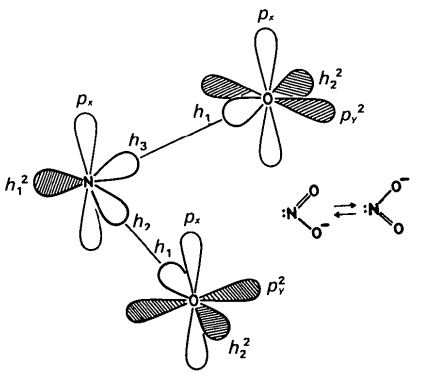

Fig. 4. A simple molecular orbital model of NO_2^-. The shaded portions indicate lone-pair orbitals.

Table 9. *Effect of the series termination on the difference synthesis*

The values of the deformation-density peak heights are multiplied by 10^2 (e Å^{-3}).

		d^+		d^-		
S_{max}	No.*	obs.	calc.	obs.	calc.	θ†
2·72	992	169	168	−79	−97	+7°
2·60	873	156	158	−88	−95	+5
2·50	783	146	150	−88	−93	+2
2·40	702	143	141	−92	−91	+3
2·30	623	134	132	−92	−89	−5
2·20	552	124	122	−91	−86	−5
2·00	426	101	103	−86	−78	0
1·80	317	85	83	−72	−69	0
1·60	227	61	64	−56	−58	−3

* The number of independent reflexions used in the calculation of the difference syntheses.

† The angle of (N–O bonding peak)–N–O; positive values of this angle indicate that the peak lies outside the ONO triangle.

perpendicular to the ONO plane. The two peaks are largely elongated perpendicularly to the ONO plane, partly owing to the large thermal motion of the O atom in this direction as evidenced by a large value of U_{33} shown in Table 8. The same feature was reported for *p*-nitropyridine *N*-oxide (Coppens & Lehmann, 1976).

Fig. 6 presents a section of the difference Fourier synthesis containing the N—O axis and perpendicular to the plane of the nitro group. The peak on the N—O axis is slightly elongated, suggesting some π-bond character. This is supported by the nearly isotropic thermal motion of the N atom (see Table 8). Furthermore, a pair of positive peaks of 0·33 (7) e Å^{-3} appear above and below the N—O axis. On the other hand, two negative peaks of heights −0·41 (10) e Å^{-3} appear above and below the N atom. This means that N(p_x) is electron deficient and the O atoms possess an excess electron in the p_x orbital. These observed features may well correspond to the N—O π-bond nature illustrated in Fig. 4.

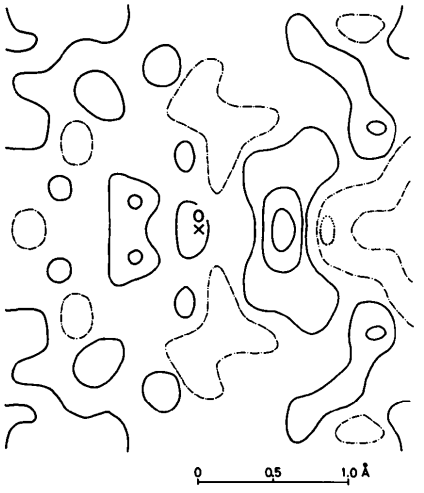

Fig. 5. Section of the difference synthesis through the O atom, showing two lone-pair peaks in the plane of the NO_2 group. The section is perpendicular to the NO_2 plane and makes an angle of about 80° to the N—O bond axis. Contours are at intervals of 0·1 e Å^{-3}.

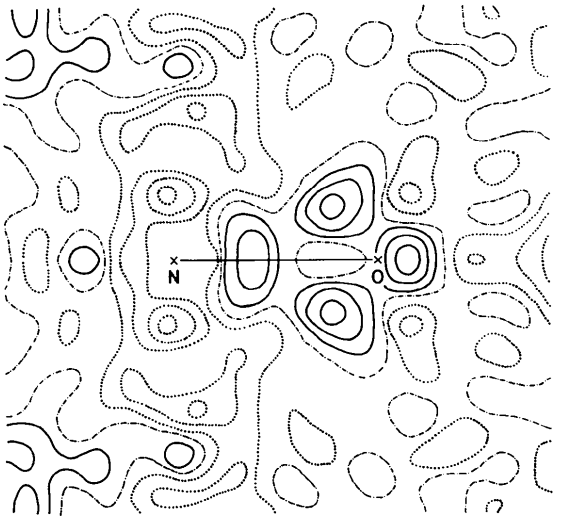

Fig. 6. Section of the difference synthesis through a N—O bond and perpendicular to the NO_2 plane. Contours are at intervals of 0·1 e Å^{-3}.

Fig. 7 presents a section of the final difference synthesis on the (100) plane through the Co atom. The lone pair N(h_1^2) of a nitro group is oriented towards the electron-deficient Co e_g orbital, to form a coordination bond. The positive peaks around the Co atom are the sections of positive regions perpendicular to the cube edges formed by eight peaks due to 3*d* electrons in t_{2g} orbitals. The Na^+ ion at the 4(*b*) site is surrounded by the broad positive region, with height 0·8 (1) e Å^{-3} on a sphere of radius 0·3 Å around it. This fact suggests some neutralization of the Na^+ ion. In fact the net charge on the Na atom obtained by charge integration is +0·6 (1) e, being independent of radius r for the range of $1{\cdot}25 \le r \le 1{\cdot}50$ Å. Neutralization of the Na atom is observed to a greater extent in the crystals of NaSCN, $NaCN.2H_2O$ and Na sulfanilate.$2H_2O$ (Bats, Coppens & Kvick, 1977). In fact, the Na···O distance of 2·7619 (7) Å is longer than those observed in $NaCN.2H_2O$ (about 2·4 Å).

Asphericity shift

At the final stage of the refinement, the discrepancies between the positional parameters based on the high-order reflexions ($\sin\theta/\lambda \ge 0{\cdot}7$ Å^{-1}) and those based on all the reflexions were less than their standard deviations for the O atom, but nearly twice their standard deviations for the N atom. Owing to the bonding effect of Co—N, the atomic parameter of the N atom is biased and shifted towards the Co atom in the conventional refinement. These asphericity shifts were not observed for the O atom. The study of *p*-nitro-

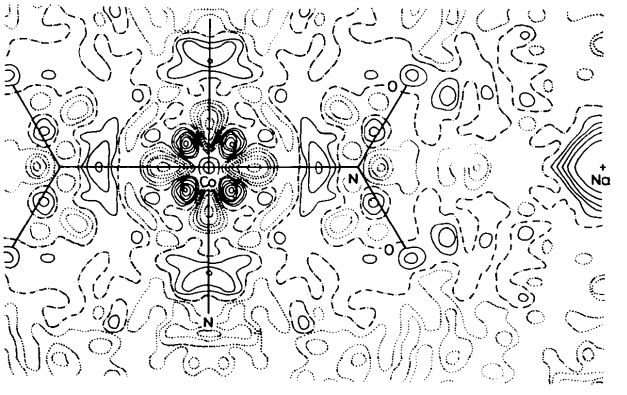

Fig. 7. Section of the difference synthesis on the (100) plane. Contours are at intervals of 0·15 e Å^{-3}.

pyridine *N*-oxide (Coppens & Lehmann, 1976), however, showed that the N—O bonds are about 0·007 Å longer from the X-ray conventional refinement than from the neutron analysis, and for the X-ray high-order refinement the remaining discrepancy amounts to 0·002 Å.

In order to see whether or not the appearance of the lone-pair peak $O(h_2^2)$ is an artifact sensitive to small shifts in the atomic position, the positional parameters of the O atom were shifted artificially by about three standard deviations of N—O bond distance (0·003 Å) towards or backwards from the N atom. The resulting maps presented in Fig. 8 show drastic changes in the mysterious peak near the O atom, but the other peaks are not at all affected. Accordingly the peak near the O atom on the extension of the N—O bond may be insignificant.

Series-termination effect

The deformation density was calculated for various values of $S_{max} = (2 \sin \theta/\lambda)_{max}$, in order to investigate the effect of series termination. The observed peak heights are plotted in Fig. 9 as a function of $(\sin \theta/\lambda)_{max}$. Surprisingly the positive peak arranged at the apices of a cube around the Co nucleus (d^+) shows a straight increase. In contrast to this, the negative trough located on the Co—N bond (d^-) shows a decrease in depth. It is to be noted that not only the positive but also the negative peaks are affected by the series-termination effect. Generally the height of the bonding and lone-pair peaks tends to increase. The mysterious peak $O(h_2^2)$ and the π-bond peak in the N—O bond begin to appear at $\sin \theta/\lambda = 1{\cdot}1$ Å^{-1} and increase rapidly in the same way.

Recently, Lehmann & Coppens (1977) proposed a method of estimating the series-termination effect on deformation density. This simple method was used for the two peaks (d^+) and (d^-). The peak of infinite resolution was assumed to be an isotropic Gaussian distribution, $\rho(r) = \rho(0) \exp(-r^2/2\sigma_T^2)$. Observed peak heights $\rho'(0)_{obs}$ were fitted to $\rho'(0)_{calc}$ by a least-squares method: the function minimized was $R' = \{\sum [\rho'(0)_{calc} - \rho'(0)_{obs}]^2 / \sum [\rho'(0)_{obs}]^2\}^{1/2}$. The values obtained were for the peak (d^+) $\sigma_T = 0{\cdot}11$ (1) Å, $\rho(0) = 2{\cdot}3$ (1) e Å^{-3} and $R' = 1{\cdot}8\%$, and for the peak (d^-) $\sigma_T = 0{\cdot}17$ (1) Å, $\rho(0) = -1{\cdot}0$ (1) e Å^{-3} and $R' = 6{\cdot}8\%$. The results are listed in Table 9. The peak (d^+) is so sharp that even at $S_{max} = 2{\cdot}72$ Å^{-1}, it attains 72% of the peak height for infinite resolution. Under the assumption of isotropic density distributions, we can estimate the integrated density in the peaks, which is found to be 0·055 e and −0·072 e for (d^+) and (d^-), respectively. Assuming that the eight (d^+) peaks are excess electron density in t_{2g} orbitals ($3\Delta t_{2g} = 0{\cdot}055 \times 8$ e) and the six (d^-) peaks being a deficiency in e_g orbitals ($2\Delta e_g = -0{\cdot}072 \times 6$ e), the difference of $3d$ electron population between a t_{2g} and an e_g orbital ($\Delta t_{2g} - \Delta e_g$) is calculated to be 0·36 e.

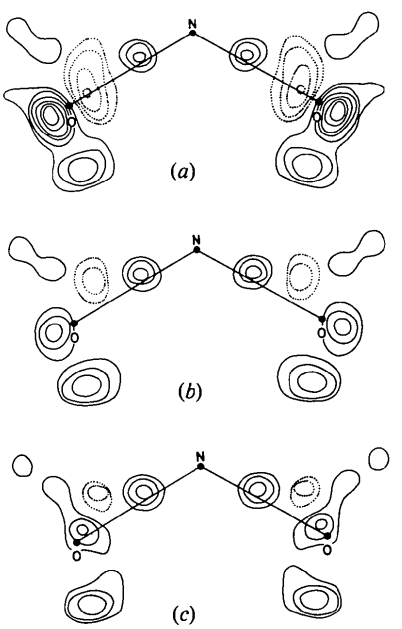

Fig. 8. Change in the deformation density in the NO_2 plane with the O atom (*a*) moved by 0·003 Å towards the N atom, (*b*) fixed at the original position, and (*c*) moved by 0·003 Å backwards from the N atom.

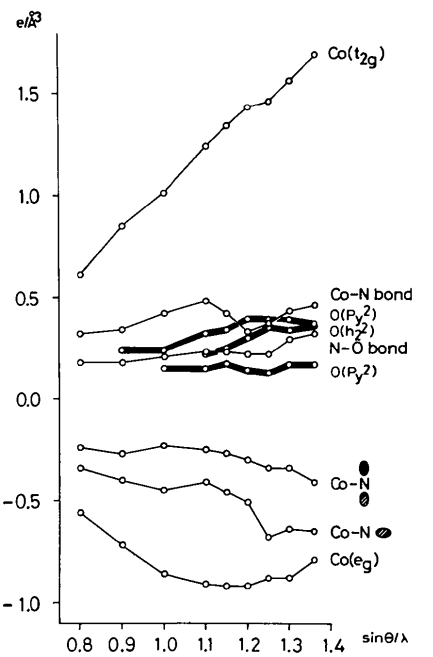

Fig. 9. The maximum value of the deformation density as a function of the cut-off value $(\sin \theta/\lambda)_{max}$ in the Fourier summation. The results for the lone-pair peaks of the O are represented by the heavy lines. The result of the π-bond peak on the N—O bond overlaps for the most part that of the $O(h_2^2)$ lone-pair peak and was not drawn.

Table 10. *Calculated electron populations in the atomic orbitals*

								Total	Charge
N	2*s*	1·638	$2p_x$*	0·829	$2p_{y'}$	1·432	$2p_{z'}$	1·026	4·926	+0·07 e
O	2*s*	1·833	$2p_x$	1·585	$2p_y$	1·971	$2p_z$	1·148	6·537	−0·54

* *x*, *y* and *z* are defined as in Fig. 4. *y'* refers to the O—O direction and *z'* is perpendicular to *x* and *y'*.

Theoretical deformation-density map for NO_2^-

Using the positional parameters obtained by the X-ray study, theoretical difference electron-density contours in the NO_2^- ion were calculated by the CNDO/2 molecular orbital method (Ito, 1975). The effect of the crystal field as well as that of coordination to the Co atom were not taken into account. The electron populations of the atomic orbitals are listed in Table 10. These values show that the N atom is almost neutral and the O atoms are negative (−0·5 e). The populations of p_x orbitals in the O atoms are twice that in the N atom. These results agree qualitatively with those obtained by the population analysis shown in Table 4 and the observed deformation-density map given in Fig. 6. The calculated deformation map is shown in Fig. 3(*b*). In this map the effect of the thermal vibration was not taken into account, and the subtracted densities were calculated on the basis of the spherical atoms with effective charges listed in Table 10. The lone-pair peaks for $N(h_1^2)$ and $O(p_y^2)$ appear on the map; however, in the N—O bonding region no positive peaks are observed, since the charge density distribution corresponding to six out of the nine occupied molecular orbitals gives a negative contribution in the N—O bonding region. An *X*—*N* difference map of non-coordinated NO_2^- was obtained in crystals of $NaNO_2$ (Ito & Shibuya, 1977), and it shows a negative N—O bonding region in agreement with this theoretical map. Accordingly the peak observed on the N—O axis in the present study may represent the redistribution of charge density owing to coordination to the Co atom.

The authors wish to express their gratitude to Dr H. Morita for his kind assistance in molecular orbital calculations by the CNDO/2 method. The calculations were carried out on the FACOM 230-48 computer of this Institute and the HITAC 8800/8700 computer at the Computer Centre of the University of Tokyo. Part of the cost of this research was met by a Scientific Research Grant from the Ministry of Education to which the authors' thanks are due.

References

BATS, J. W., COPPENS, P. & KVICK, Å. (1977). *Acta Cryst.* B**33**, 1534–1542.

COPPENS, P. & LEHMANN, M. S. (1976). *Acta Cryst.* B**32**, 1777–1784.

CRUICKSHANK, D. W. J. (1956). *Acta Cryst.* **9**, 754–756.

CULLEN, D. L. & LINGAFELTER, E. C. (1971). *Inorg. Chem.* **10**, 1264–1268.

FERRARI, A., CAVALCA, L. & COGHI, L. (1955). *Gazz. Chim. Ital.* **85**, 273–287.

FUKAMACHI, T. (1971). Tech. Rep. B12. Institute for Solid State Physics, Univ. of Tokyo.

ITO, T. (1975). *Bull. Chem. Soc. Jpn*, **48**, 3035–3038.

ITO, T. & SHIBUYA, I. (1977). *Acta Cryst.* A**33**, 71–74.

IWATA, M. (1977). *Acta Cryst.* B**33**, 59–69.

IWATA, M. & SAITO, Y. (1973). *Acta Cryst.* B**29**, 822–832.

JOESTEN, M. D., TAKAGI, S. & LENHERT, P. G. (1977). *Inorg. Chem.* **16**, 2680–2685.

LEHMANN, M. S. & COPPENS, P. (1977). *Acta Chem. Scand. Ser. A*, **31**, 530–534.

PAULING, L. (1960). *The Nature of the Chemical Bond.* 3rd ed. Ithaca: Cornell Univ. Press.

STEVENS, E. D. & COPPENS, P. (1975). *Acta Cryst.* A**31**, 612–619.

TORIUMI, K., OZIMA, M., AKAOGI, M. & SAITO, Y. (1978). *Acta Cryst.* B**34**, 1093–1096.

TORIUMI, K. & SAITO, Y. (1978). *Acta Cryst.* B**34**, 3149–3156.

WEISS, R. J. (1966). *X-ray Determination of Electron Distributions.* Amsterdam: North-Holland.